Contract No:

This document was prepared in conjunction with work accomplished under Contract No. 89303321CEM000080 with the U.S. Department of Energy (DOE) Office of Environmental Management (EM).

Disclaimer:

SRNL-MS-2023-00237

SiC based photon counting detector for scintillator read-out in harsh environment applications

S. K. Chaudhuri[1], R. N. Nag[1], U. N. Roy[2], R. B. James[2], K. C. Mandal[1]*

[1]Dept. of Electrical Engineering, University of South Carolina, Columbia, SC 29208, USA.
[2]Savannah River National Laboratory, Aiken, SC 29831

BSRA
Battelle Savannah River Alliance, LLC

2nd Annual BSRA Universities Collaboration Exchange

Augusta, GA, Tuesday, June 20 – Thursday, June 22, 2023

UNIVERSITY OF South Carolina
College of Engineering and Computing

SRNL®
SAVANNAH RIVER NATIONAL LABORATORY

Introduction

- X- and γ-ray detection rely heavily on scintillation detectors which generate optical signals upon interaction with incident radiation.
- Si-Photomultipliers (SiPMs) are becoming the most promising solid-state alternative to the conventional photomultiplier tubes as a scintillator readout.
- Due to the low bandgap energy of silicon (1.1 eV), the dark count rate (DCR) is high even at room-temperature, increasing the minimum detectable photon counts.
- This high DCR in SiPMs limits their applications, especially in harsh environments and at higher temperature operation.
- 4H-SiC based photon counting detector operating at zero applied bias will be ideal for harsh environment applications.

Introduction

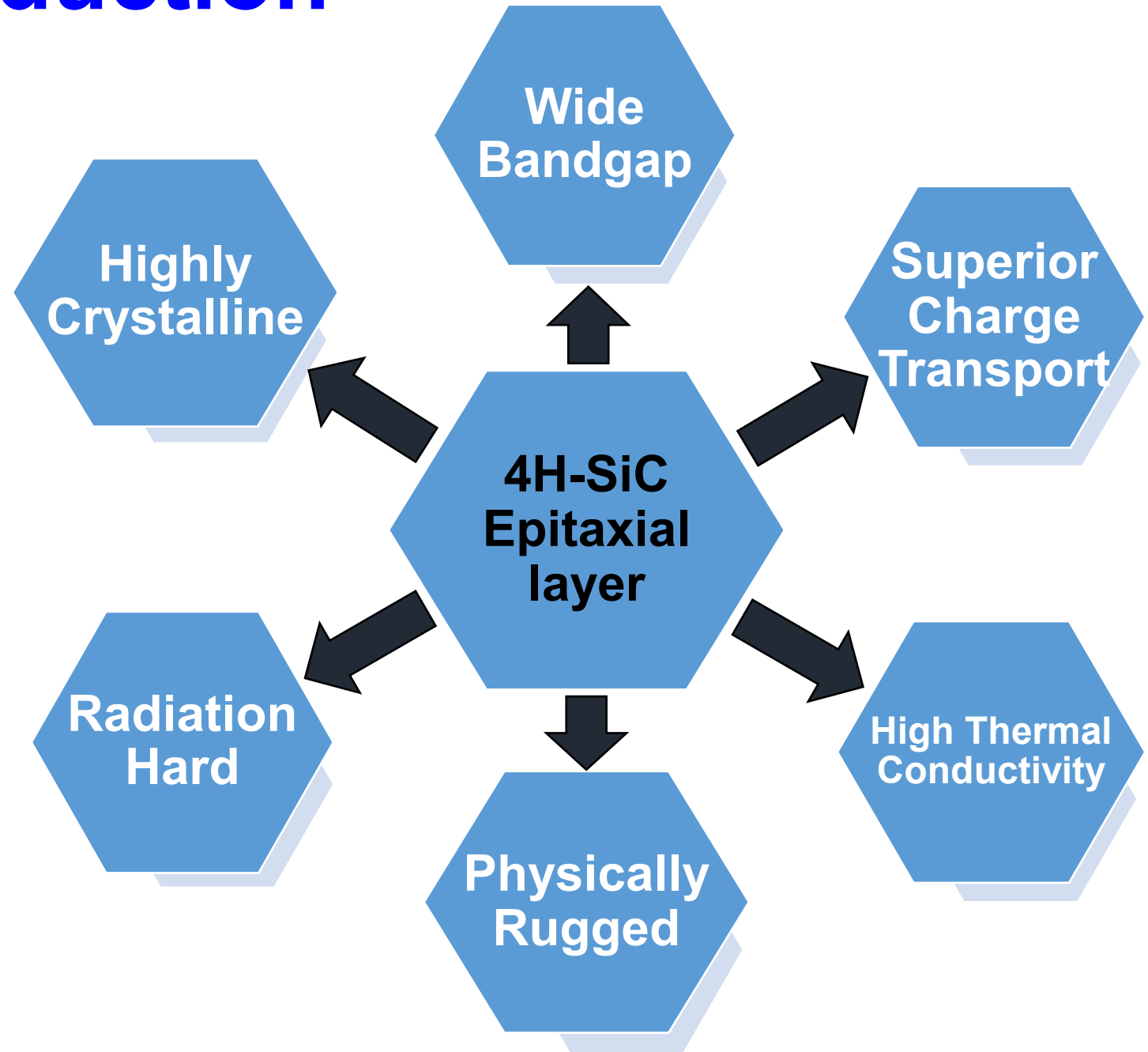

1. K. C. Mandal, S. K. Chaudhuri, F. H. Ruddy "High-resolution alpha spectrometry using 4H-SiC detectors: A review of the state-of-the-art," IEEE Trans. Nucl. Sci. **70**(5), pp. 823-830, 2023.
2. S. K. Chaudhuri and K. C. Mandal, (2022) "Radiation detection using n-type 4H-SiC Epitaxial Layer Surface Barrier Detectors," in *Advanced Materials for Radiation Detection* Ed. K. Iniewski, pp. 183-209, *Springer, Cham.*

Introduction

Physical and electrical properties of 4H-SiC

Bandgap	3.27 eV
Thermal Conductivity	4.9 W/cm/K
Electron Mobility	1020 $cm^2/V/s$
Saturation Drift Velocity	2×10^7 cm/s
Breakdown Field	3 MV/cm
Displacement Threshold	22 – 35 eV
Electron-Hole Pair Creation Energy	7.28 eV

Introduction

Applications of 4H-SiC devices

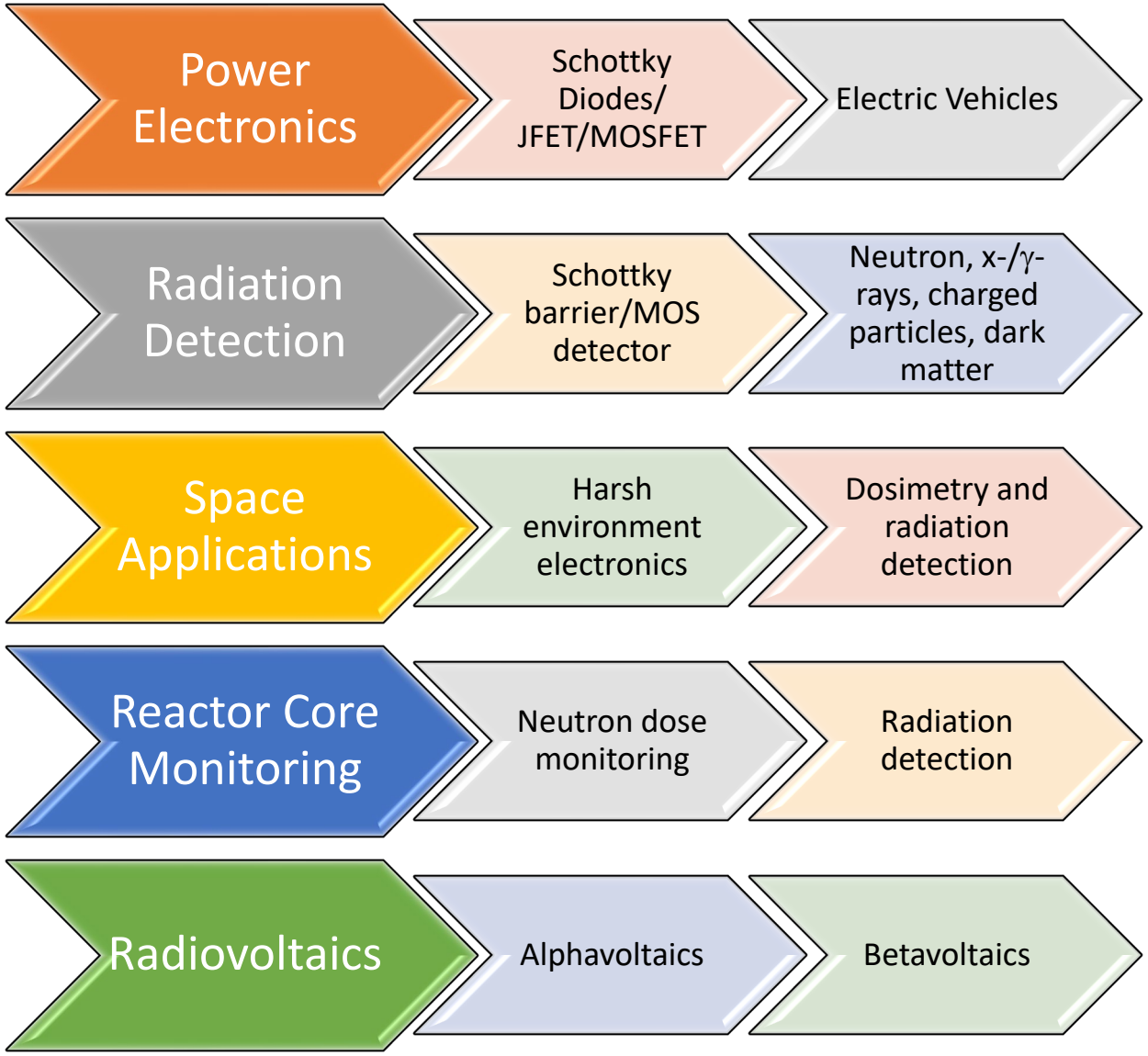

4H-SiC Epitaxial Layer

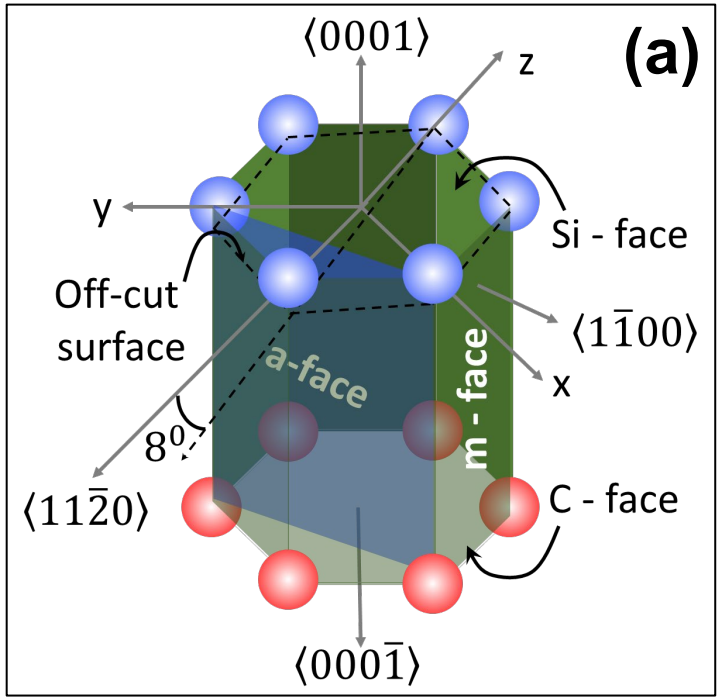

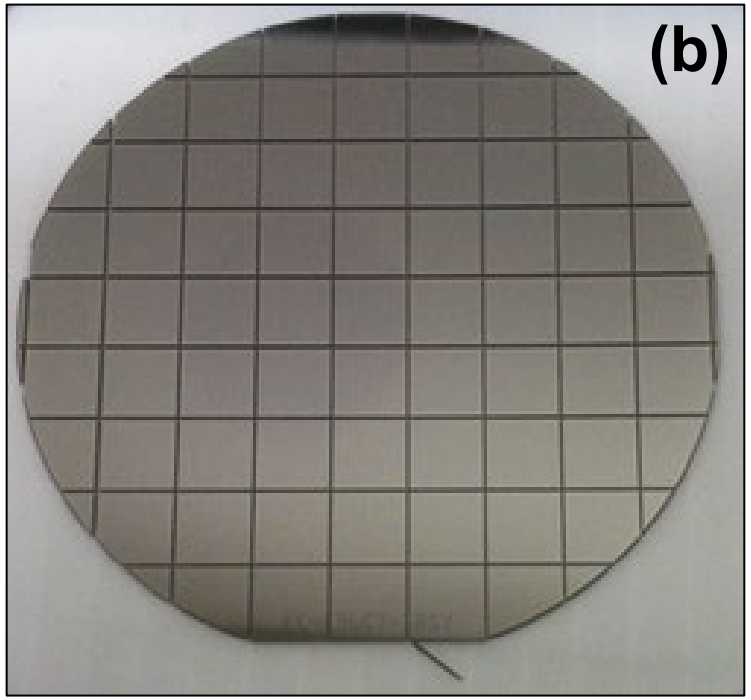

(a) Crystal planes and crystallographic directions in the 4H-SiC polytype.
(b) A 4 inch 250 µm thick detector grade n-type 4H-SiC epitaxial layer.

- The epilayers are grown on the (0001) face of a 100 mm diameter, 350 µm thick 4H-SiC conductive substrate (0.015–0.028 Ω.cm).
- The substrates were off-cut by 4-8° toward the ⟨11$\bar{2}$0⟩ direction to minimize formation 3C-polytype.
- A very low average areal micropipe density (MPD) of 0.11 cm^{-2} was found.
- The epilayers have shown ultra-low concentration of lifetime killer defects such as $Z_{1/2}$ and $EH_{6/7}$ centers.

J. W. Kleppinger, S. K. Chaudhuri, R. Nag and K. C. Mandal, J. Cryst. Growth, 583, 126532, 2022.

4H-SiC Detector Fabrication

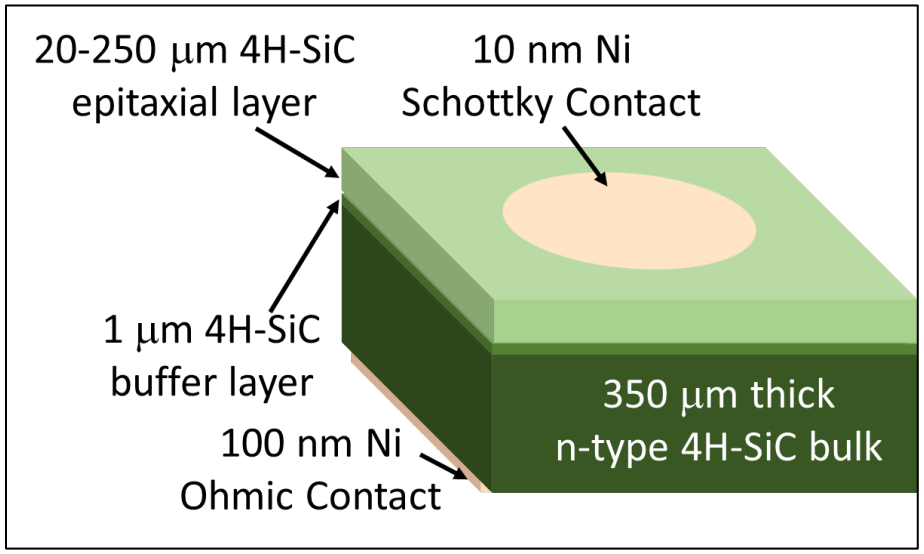

Schematic diagram of 4H-SiC radiation detector.

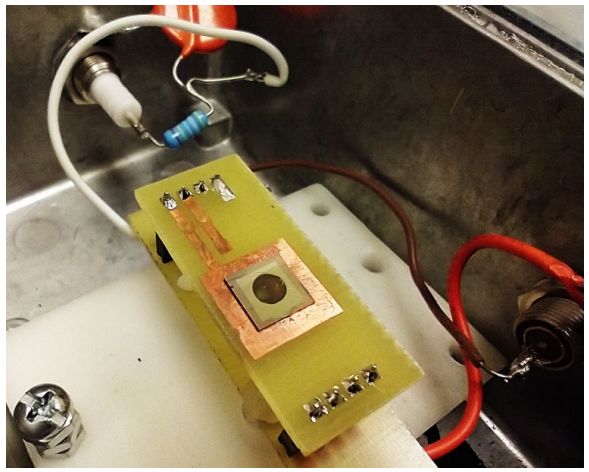

Photograph of a 4H-SiC Schottky barrier detector.

- The 4H-SiC epilayer wafers are diced into 8 × 8 mm^2 samples.
- The wafers are cleaned using an RCA method followed by a HF acid etching to remove any native oxide layer.
- Thin (10 -20 nm) nickel contacts are deposited on the epilayer (Si-face) to obtain Schottky contact for the Schottky barrier detectors (SBD).
- Thick Ni contacts (80 nm) are deposited on the bulk (C-face) side to obtain Ohmic back contacts.

S. K. Chaudhuri, R. Nag, and K. C. Mandal, IEEE Electron Device Lett. **44**(5), pp. 733-736, 2023

Detector characterization

- Current-voltage (*I*-*V*) characteristics to determine the junction characteristics.
- Capacitance-voltage (*C*-*V*) characteristics to determine the junction characteristics and effective doping concentration.
- Pulse-height spectroscopy to characterize the radiation response and charge transport properties.
- Defect characterization – Type, concentration, capture cross-section.
- Correlation of defect parameters with device parameters.

J-V / *C-V* Analysis

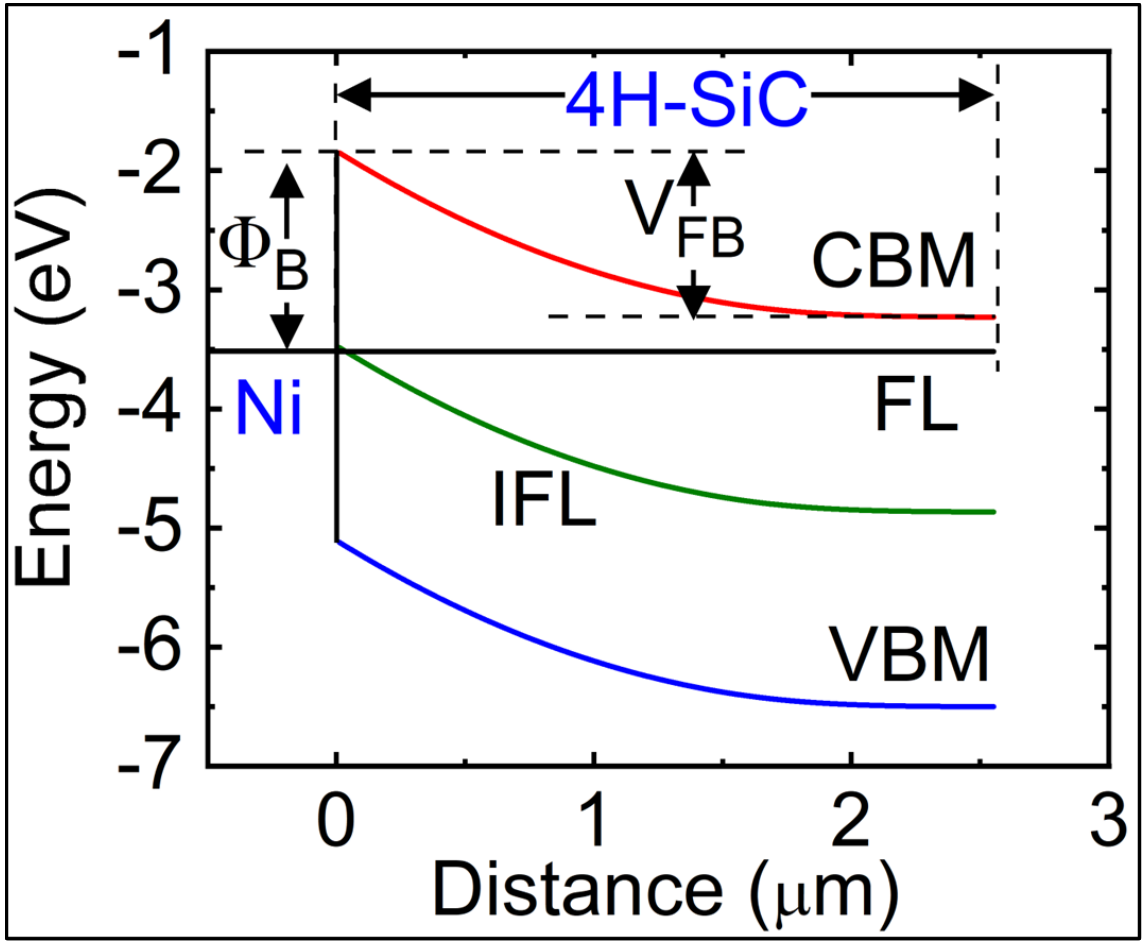

Band diagram for a Ni/(n)4H-SiC Schottky barrier detector.

K. C. Mandal, J. W. Kleppinger, and S. K. Chaudhuri, Micromachines, 11(3), 254, 2020.

J-V Characteristics

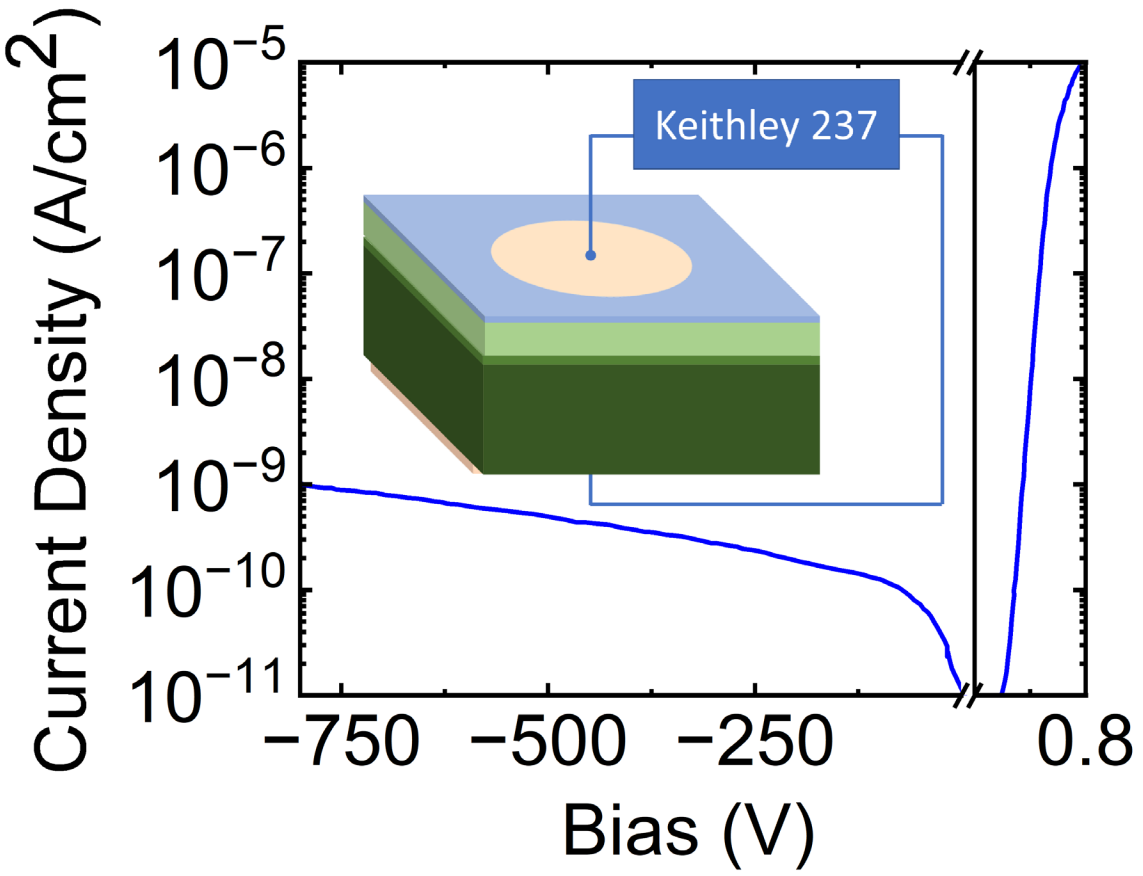

J-V characteristics of a 250 μm thick Ni/(n)4H-SiC SBD.

J. W. Kleppinger, S. K. Chaudhuri, O. Karadavut, and K. C. Mandal, J. Appl. Phys., 129, 244501, 2021.

C-V Characteristics

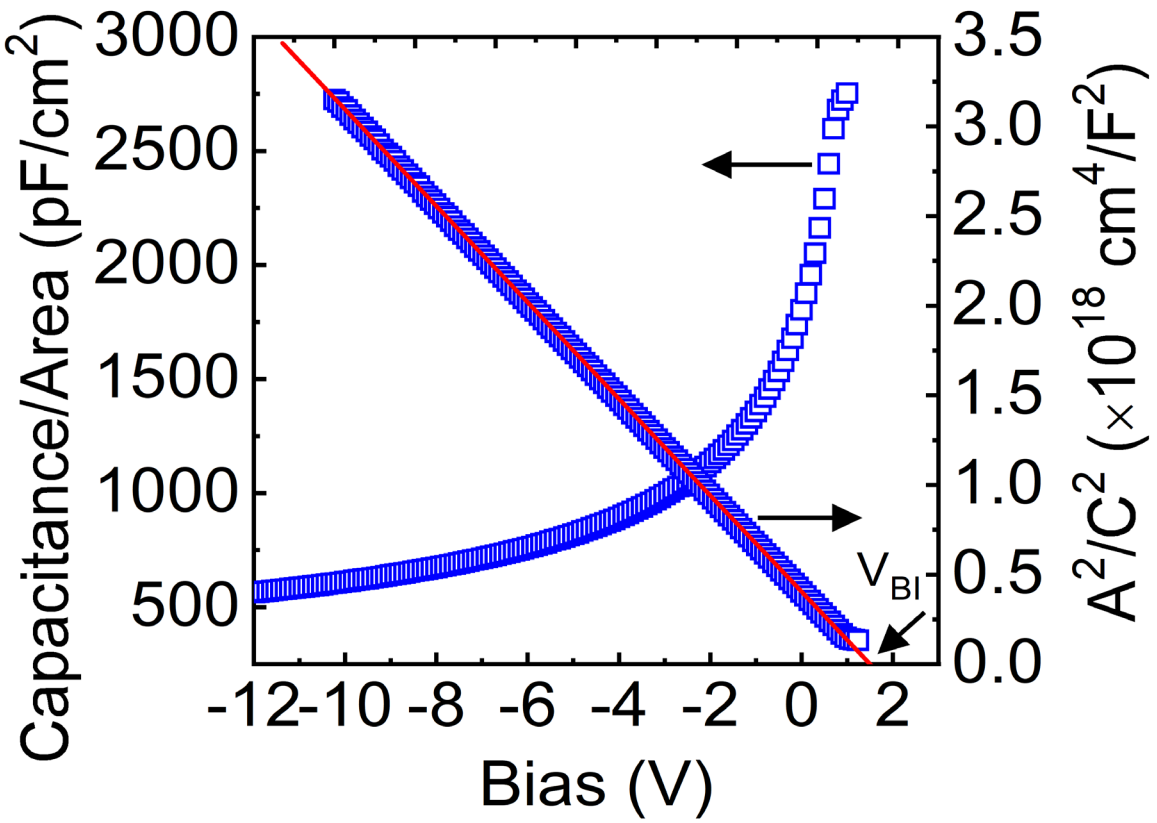

C-V characteristics of a 250 μm thick Ni/(n)4H-SiC SBD.

J. W. Kleppinger, S. K. Chaudhuri, O. Karadavut, and K. C. Mandal, J. Appl. Phys., 129, 244501, 2021.

Pulse height spectroscopy

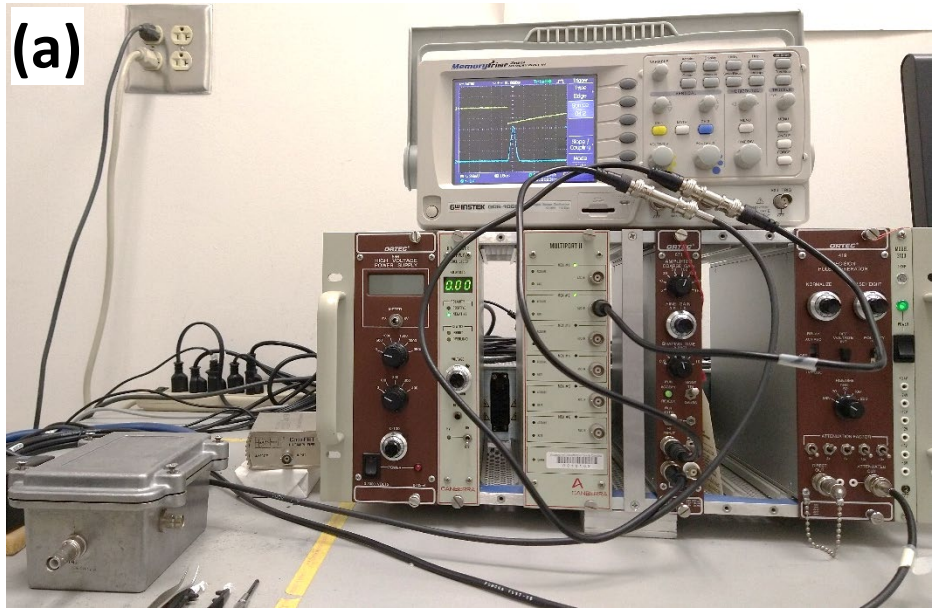

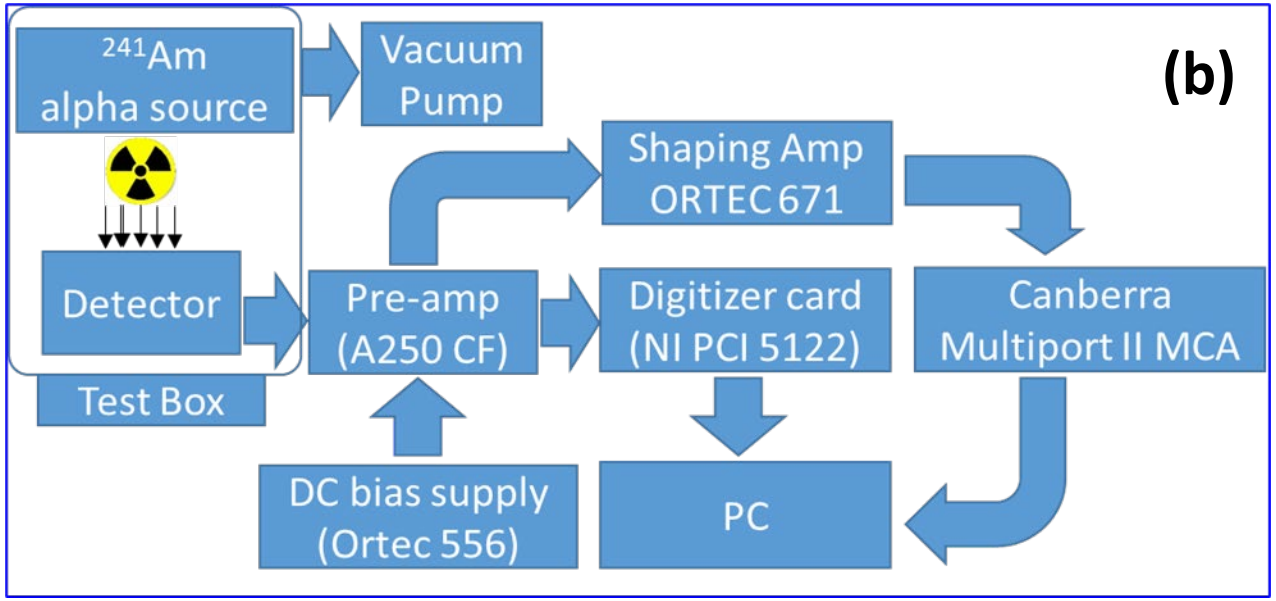

(a) Analog benchtop alpha-spectrometer at USC **(b)** Schematic of the spectrometer set up.

- An analog benchtop alpha spectrometer has been used to evaluate the radiation response of the detectors.
- A 1 µCi ^{241}Am radioisotope emitting 5486 (84.5%), 5442 (13.0%), and 5388 (1.6%) keV alpha particles has been used.
- The source-detector assembly is kept in an EMI shielded test-box which was continually evacuated during the measurements.

Pulse height spectroscopy

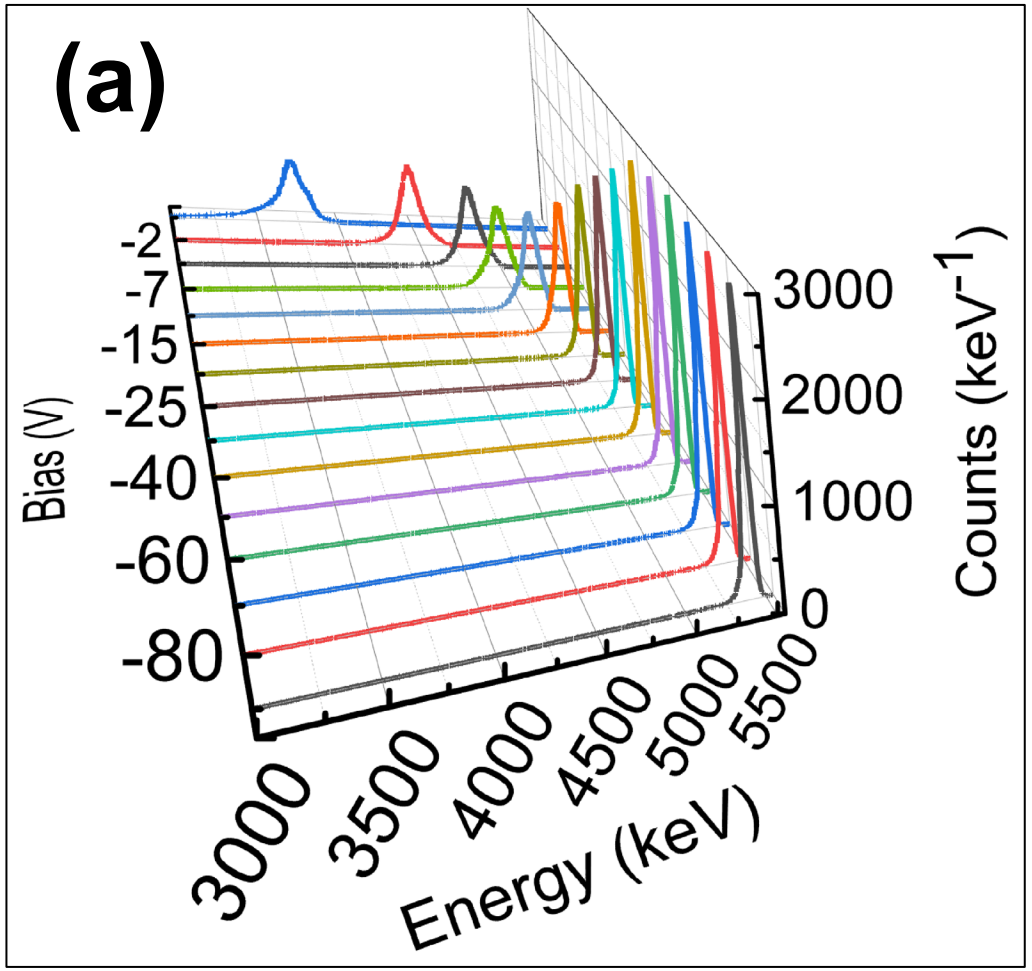

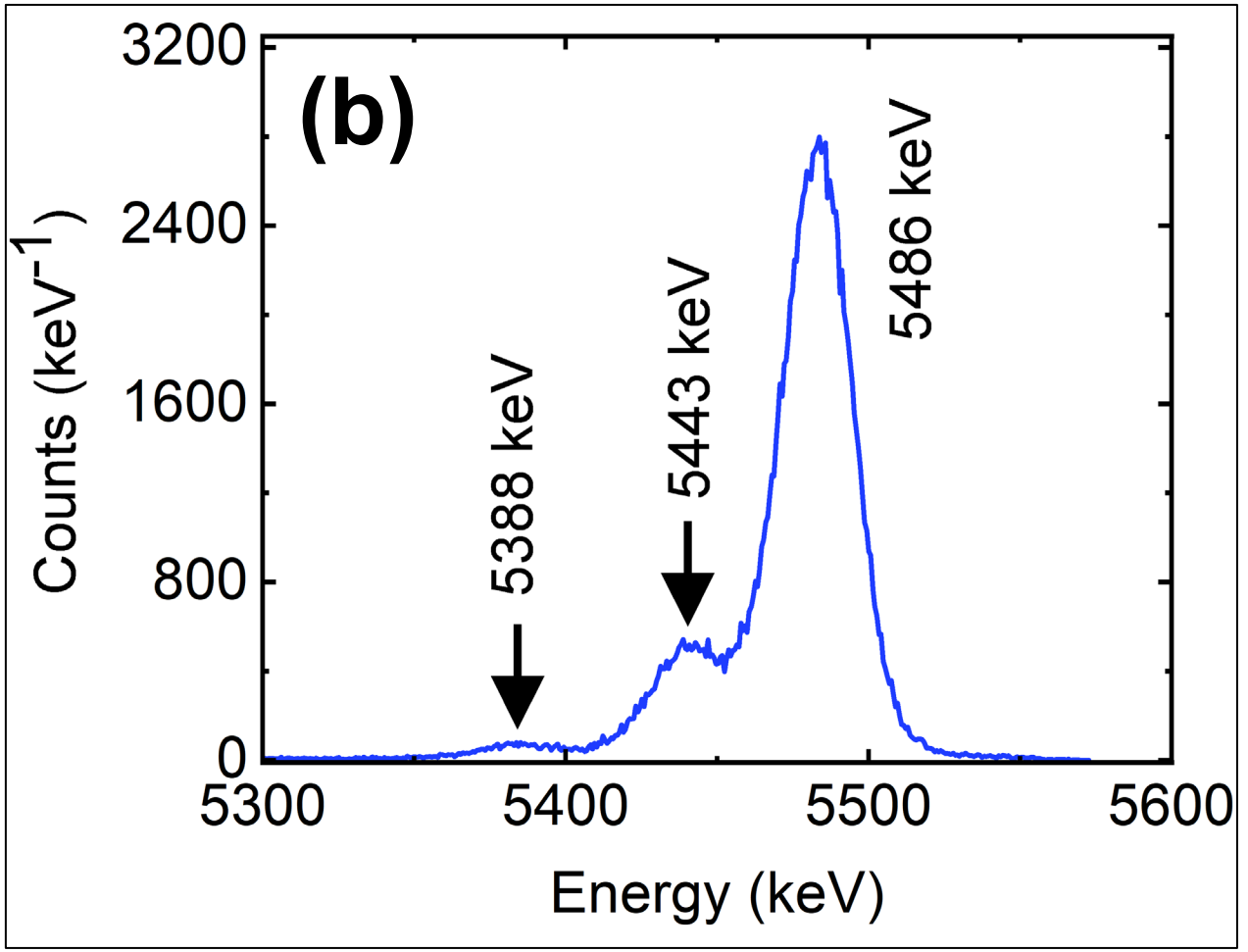

Pulse height spectrum (PHS) obtained using a ^{241}Am alpha emitter and a 250 μm thick Ni/(n)4H-SiC SBD at different bias voltages **(a)**, and at optimized condition **(b)**.

- Energy resolution - full width at half maximum (FWHM), ΔE.
- Percentage energy resolution has been expressed as $\left(\frac{\Delta E}{E_\alpha}\right) \times 100$, E_α being the measured energy of the detected peak.
- Charge collection efficiency has been defined as $\frac{E_\alpha}{5486}$, the ratio of the energy detected to the energy of the absorbed radiation.

- All the detectors exhibited robust and well resolved 5486 keV alpha peaks.
- The energy resolution was calculated to be 0.4% at 5486 keV.
- All the detectors showed 100% charge collection efficiency.

Hole diffusion length – From drift-diffusion model is given by

Range of α-particles

$$CCE = \frac{1}{E_\alpha}\int_0^{x_d}\left(\frac{dE}{dx}\right)dx + \int_{x_d}^{x_r}\left(\frac{dE}{dx}\right)\exp\left[-\frac{x-x_d}{L_d}\right]dx$$

Stopping power *Depletion width* *Minority carrier diffusion length*

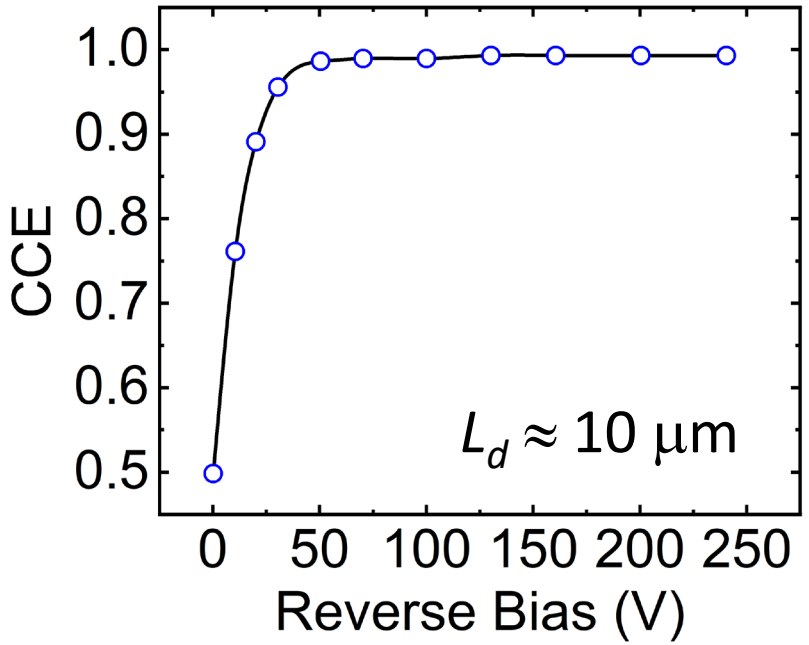

J. W. Kleppinger, S. K. Chaudhuri, O. Karadavut, R. Nag, D. L. P. Watson, D. S. McGregor, and K. C. Mandal, *IEEE Trans. Nucl. Sci.*, **69**(8), 1972-1978, 2022
M. B. H. Breese, "A theory of ion beam induced charge collection," *J. Appl. Phys.,* vol. 74, no. 6, pp. 3789-3799, Jun. 1993.

4H-SiC detector: UV detection

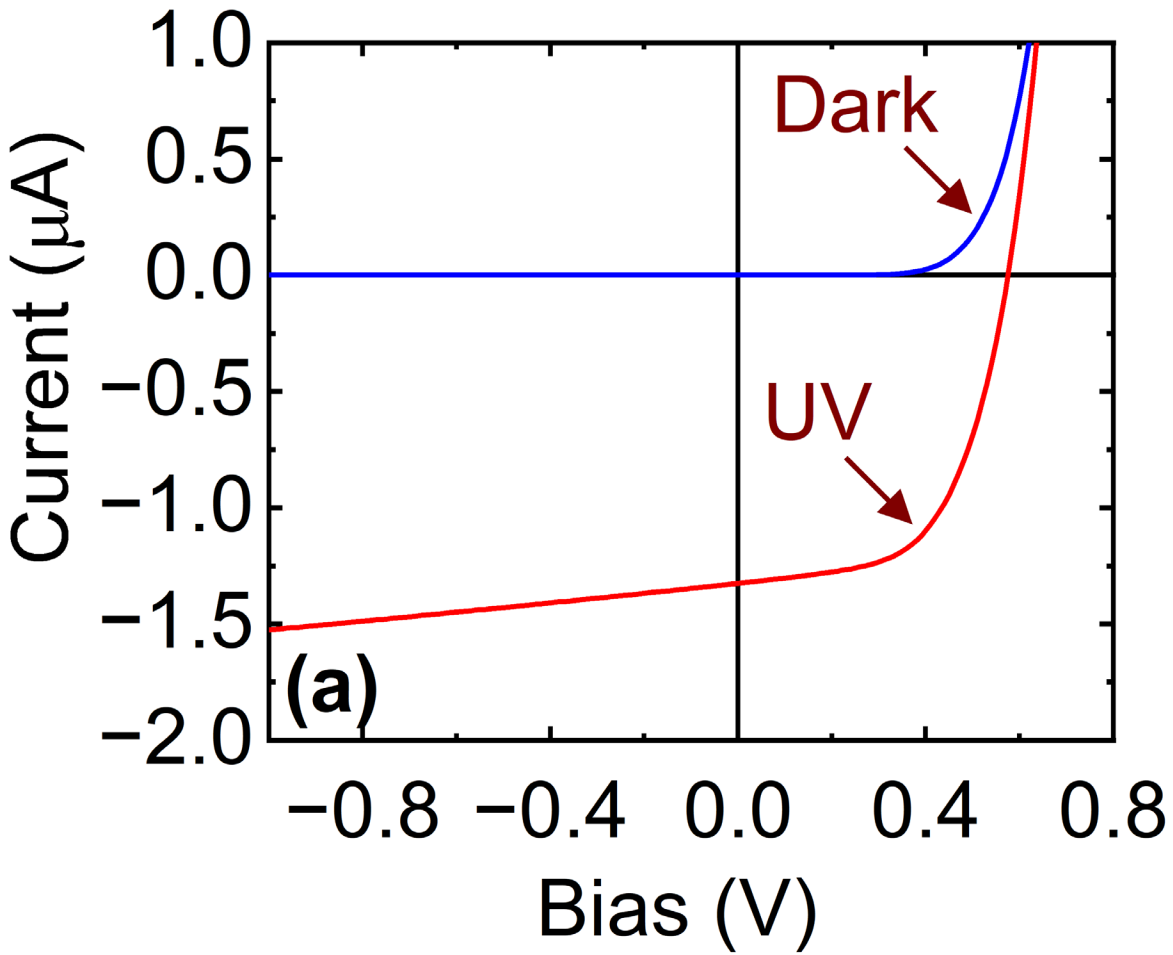

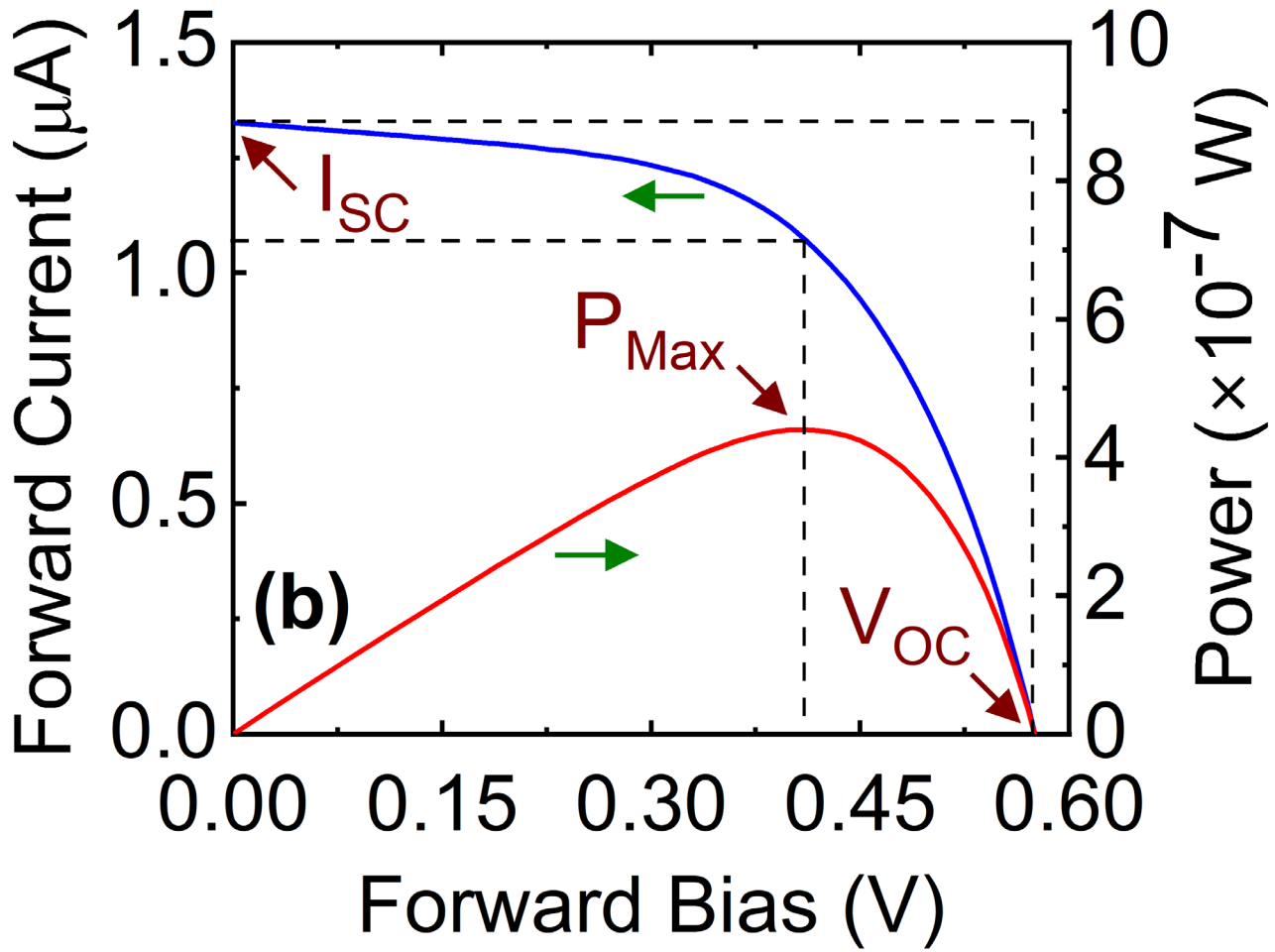

S. K. Chaudhuri, R. Nag, and K. C. Mandal, IEEE Electron Device Lett. **44**(5), pp. 733-736, 2023.

Biased and Self biased operation

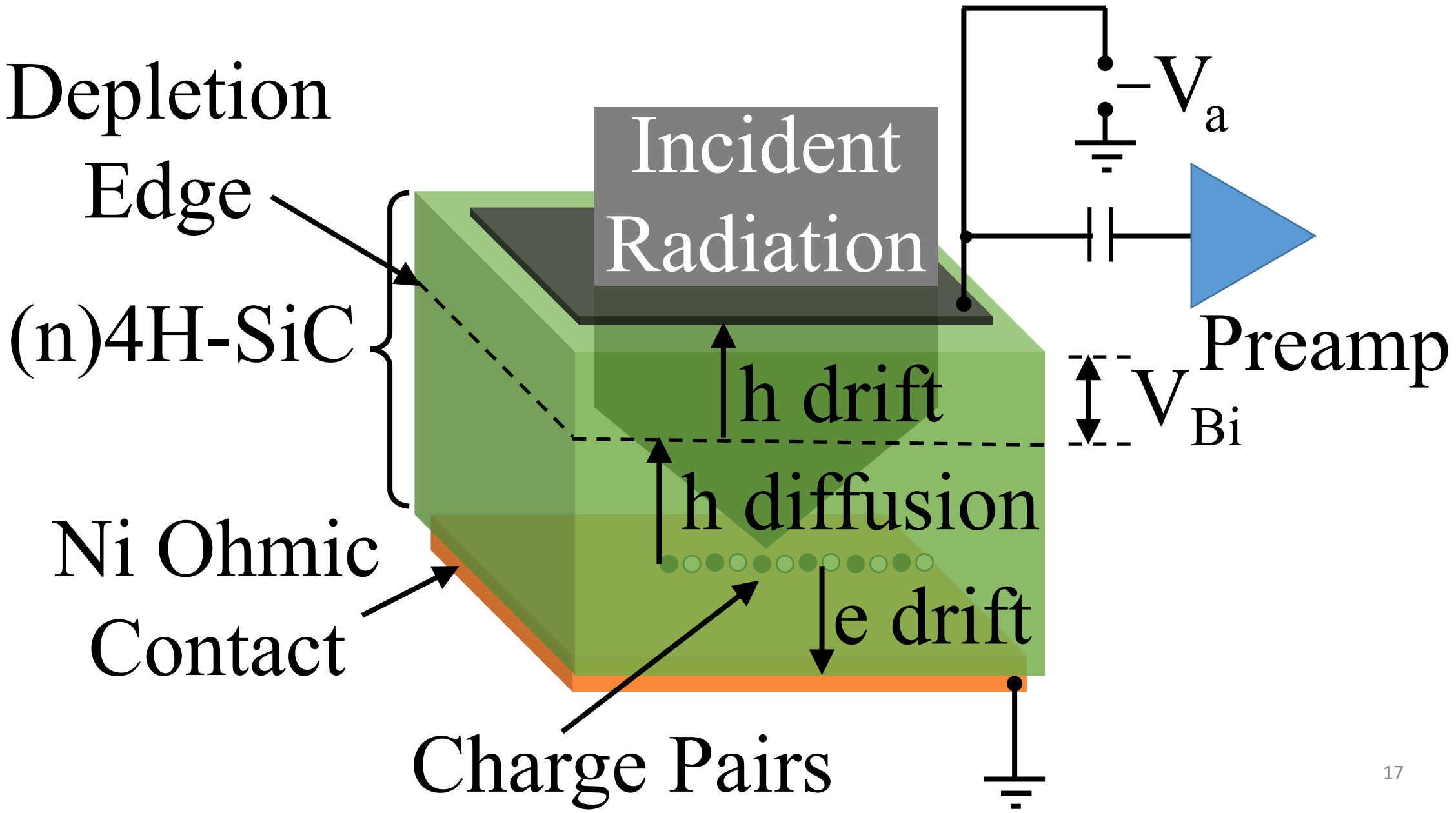

Enhanced Self biased operation: Metal-Oxide-Semiconductor (MOS) detectors

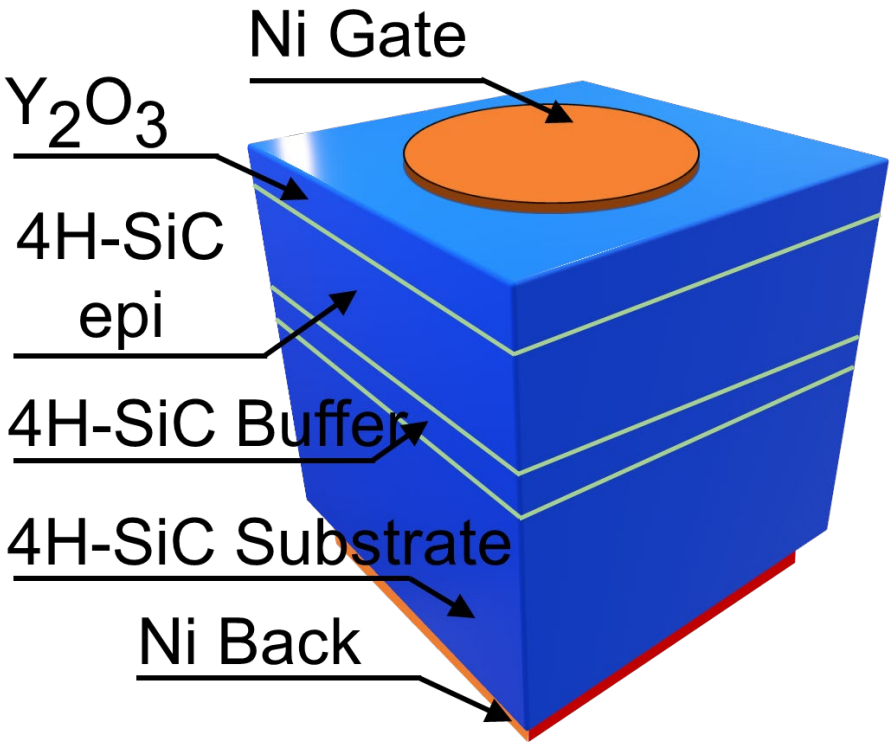

Schematic of the $Ni/Y_2O_3/(n)4H\text{-}SiC$ MOS detector.

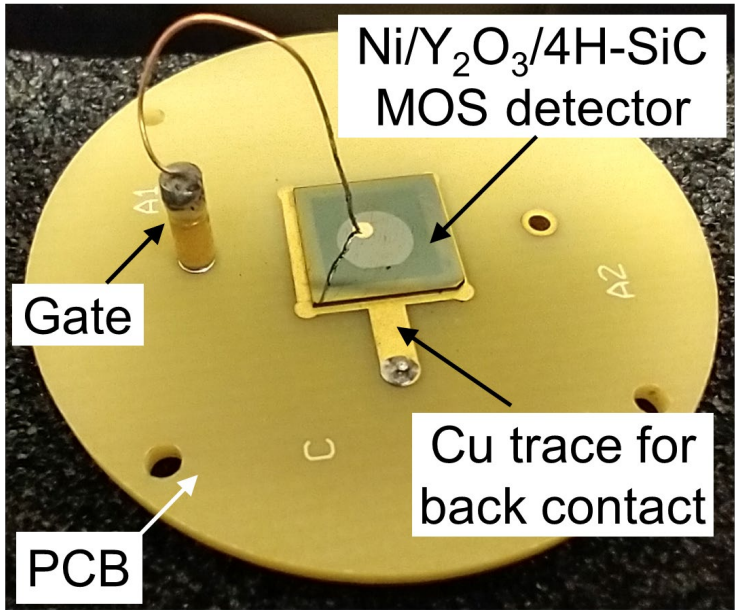

Photograph of the $Ni/Y_2O_3/(n)4H\text{-}SiC$ MOS detector.

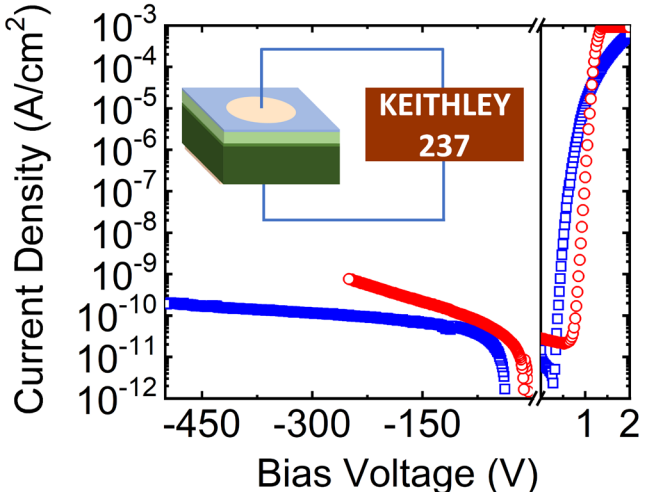

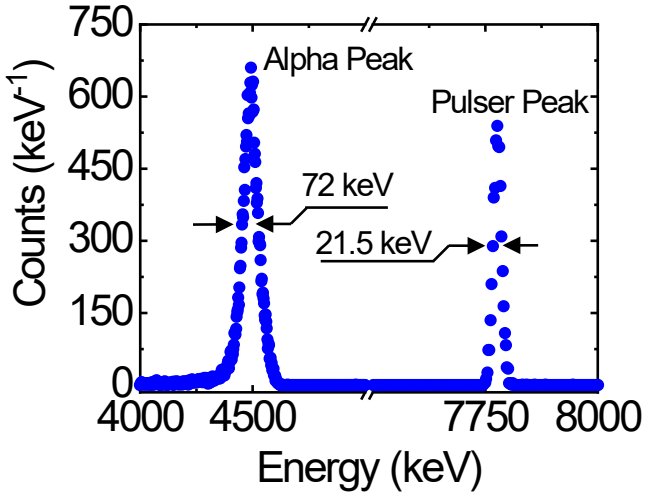

Oxide Layer Deposition

Oxide deposition facilities at USC

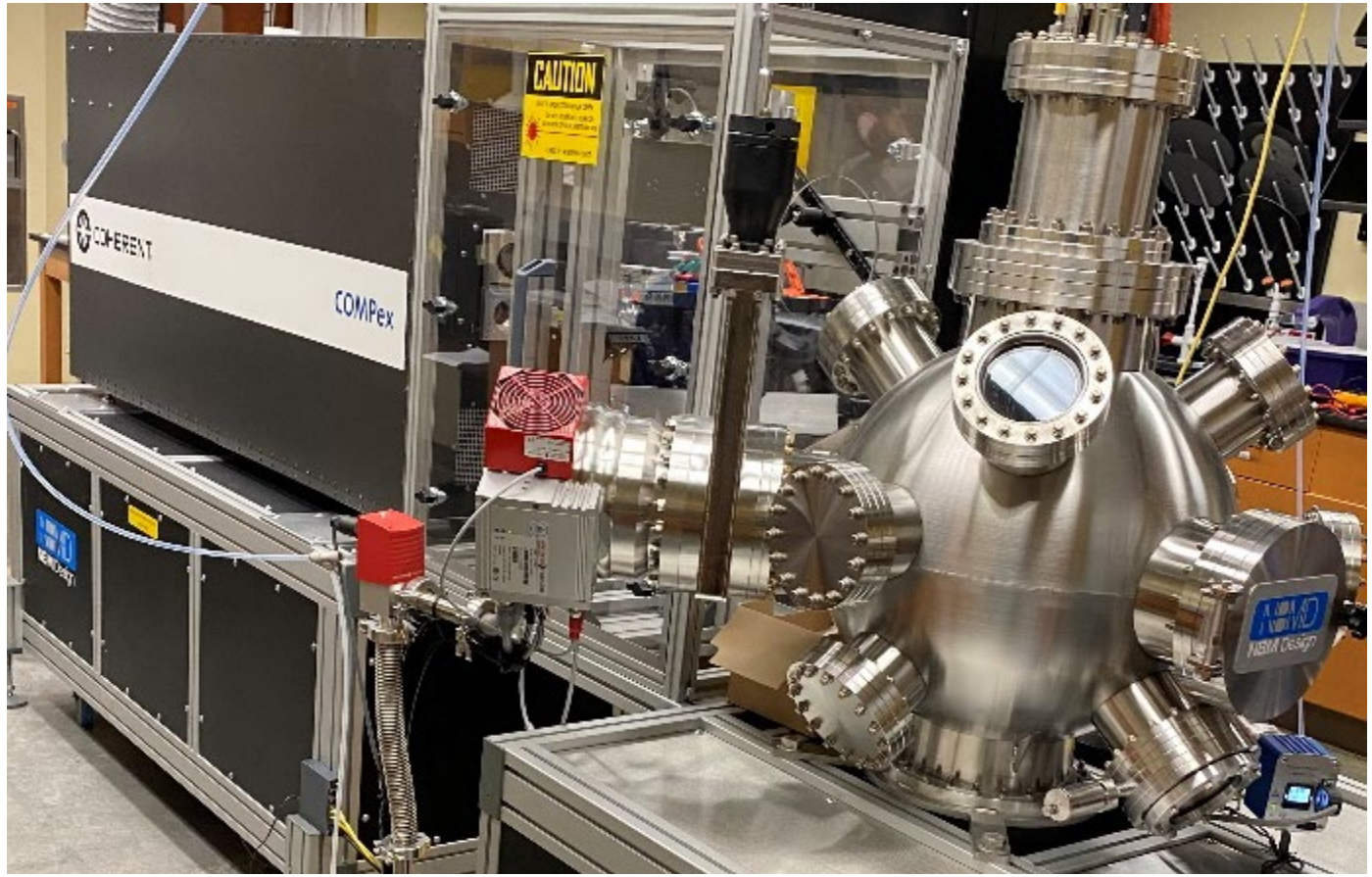

Pulsed laser deposition set-up (PLD).

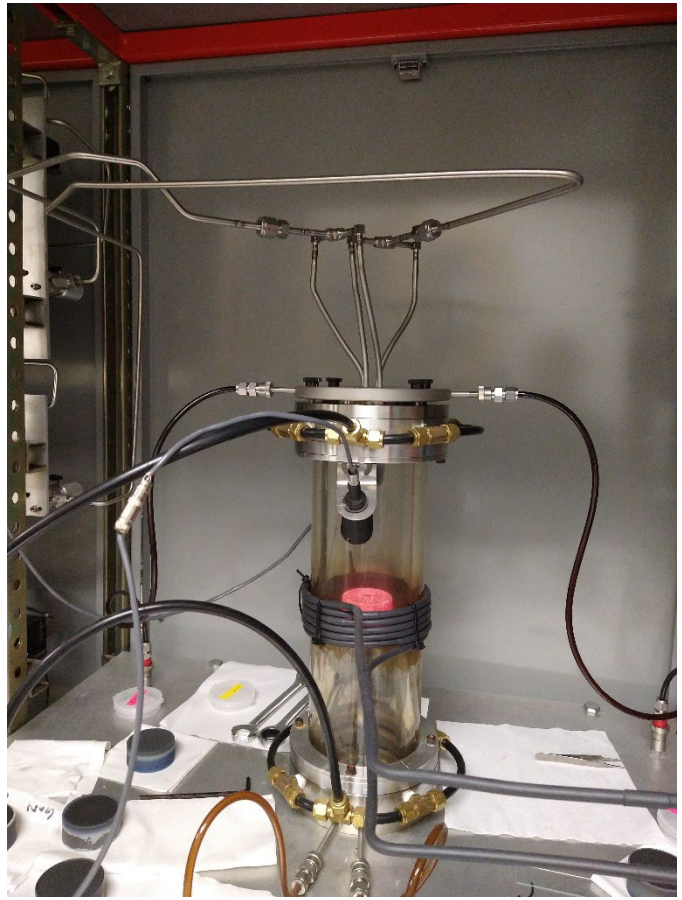

Metal organic chemical vapor deposition (MOCVD) set-up.

Comparison: device properties

Device	Epilayer Thickness (μm)	Leakage Current (nA/cm^2) @200 V	Ideality Factor	Barrier Height (eV)	Built-in potential (V)	L_d (μm)	Resolution at 0 V (%)*
Ni/4H-SiC SBD	20	0.39	1.20	1.6	2.1	18	2.5
Ni/Y_2O_3/4H-SiC MOS	20	0.08	1.07	1.5	2.1	56	1.5

*For 5486-keV alpha particles

1. S. K. Chaudhuri, J. W. Kleppinger, and K. C. Mandal, J. Appl. Phys., 128, Art. no. 114501, 2020.
2. S. K. Chaudhuri, J. W. Kleppinger, O. Karadavut, and K. C. Mandal, IEEE Electron Dev. Lett., 43(9), pp. 1416-1419, 2022.

Defect Characterization

Capacitance Mode Deep Level Transient Spectroscopy (C-DLTS)

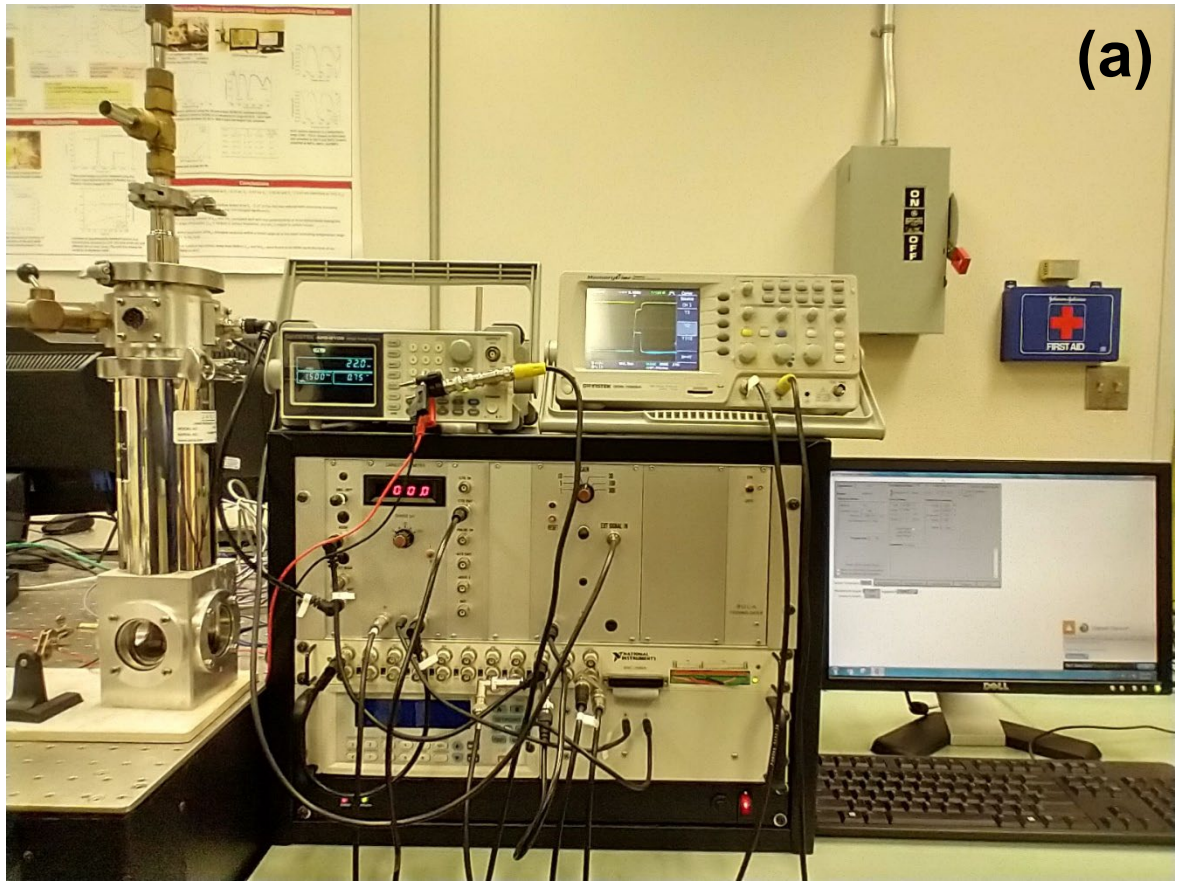

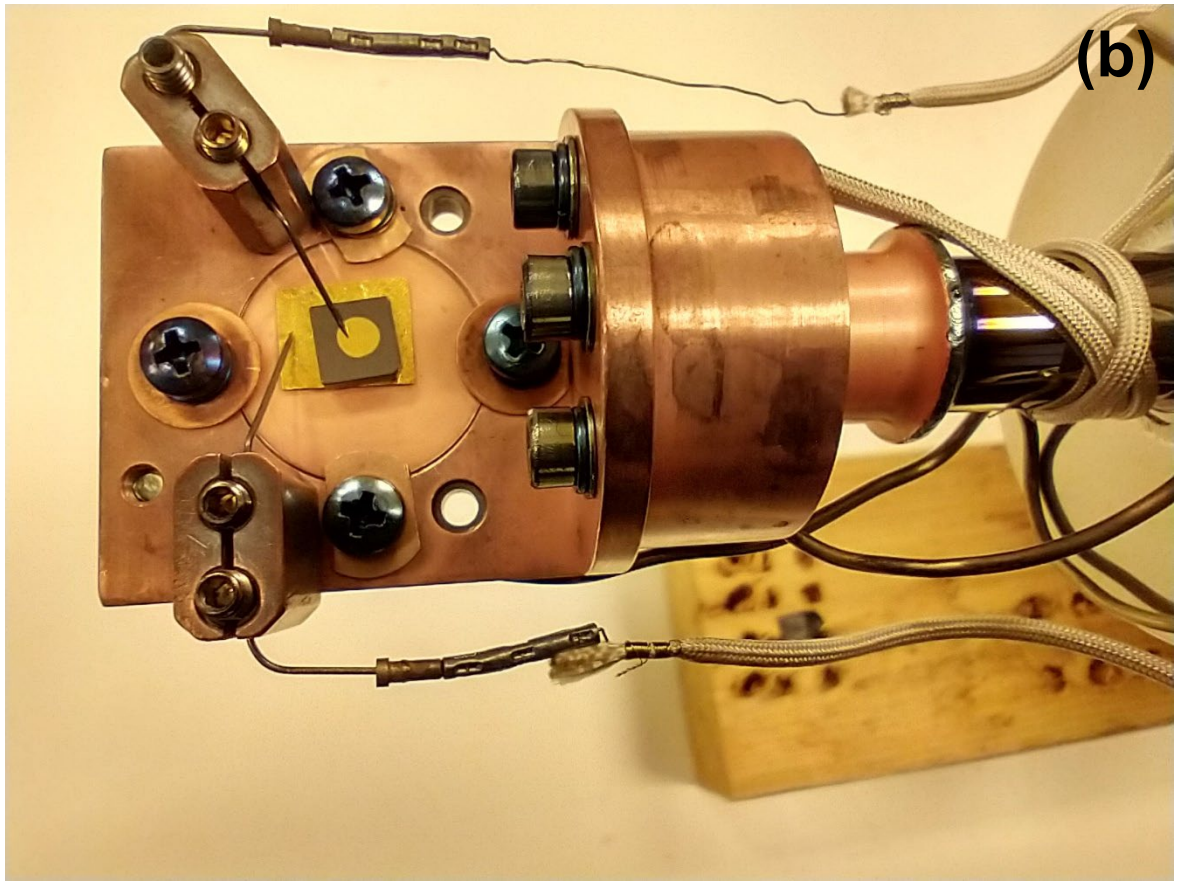

(a) A Sula Technologies DDS-12 DLTS spectrometer at USC **(b)** A detector mounted on the Janis VPF800 cryostat.

Capacitance Mode Deep Level Transient Spectroscopy (C-DLTS)

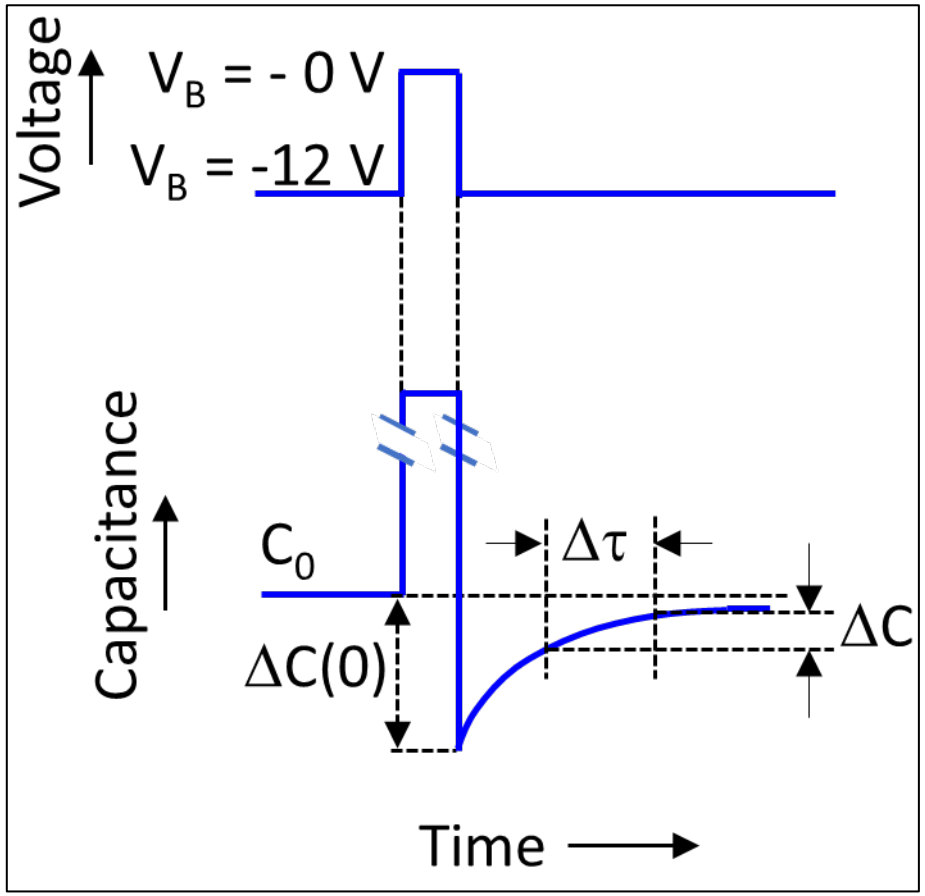

DLTS signal generation.

- Capacitance transient

$$C(t) = C_0 + \Delta C e^{-te_n}.$$

e_n is the emission rate from a trap which at resonant temperature T_m equals to $(\Delta\tau)^{-1}$.

- The emission rate is given by

$$e_n = \left(\sigma_n \langle v_{th} \rangle N_c / g\right) \exp(-(E_C - E_T)/kT)$$

$\langle v_{th} \rangle$ is the mean thermal velocity and g is the degeneracy of the trap level.

- The defect concentration N_t is given as

$$N_t = 2\left(\frac{\Delta C(0)}{C_0}\right) N_d,$$

where, $\Delta C(0)$ is the difference in capacitance before and after the filling pulse, and N_d is doping concentration.

1. D. V. Lang, J. Appl. Phys., 45, 3023, 1974.
2. S. K. Chaudhuri, O. Karadavut, J. W. Kleppinger and K. C. Mandal, J. Appl. Phys., 130, 074501, 2021.

Defect Characterization (Contd.)

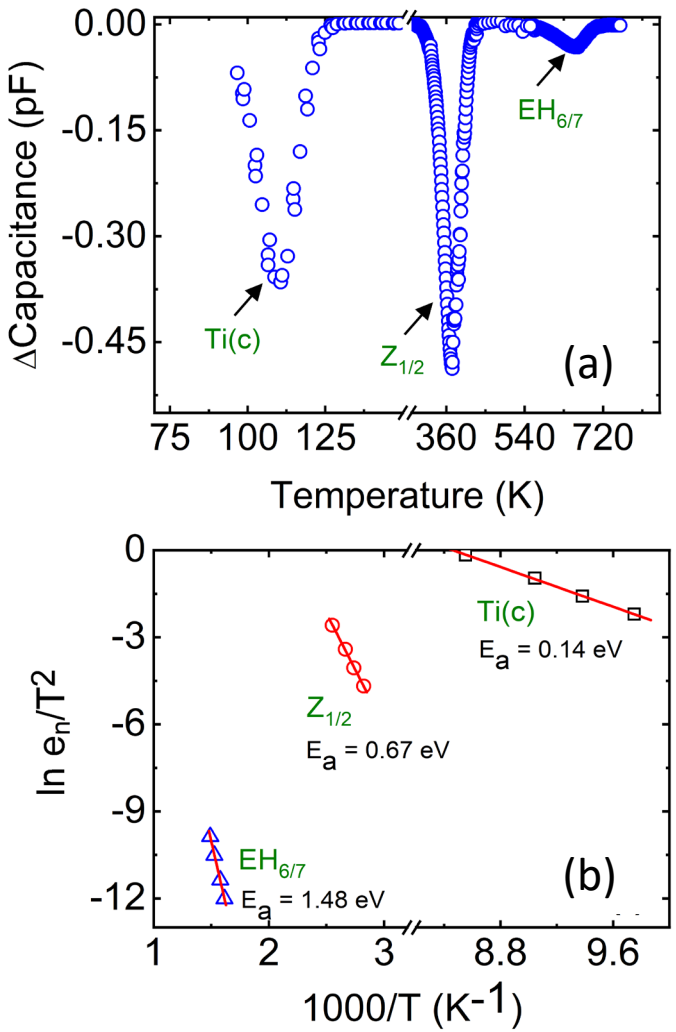

(a) DLTS spectra obtained for a 40nm/20 µm thick Ni/Y_2O_3/4H-SiC MOS detector **(b)** The corresponding Arrhenius plots.

Trap Center	Activation Energy (eV)	Concentration (cm^{-3})	Capture Cross-section (cm^2)
Ti (c)	0.14	2.03×10^{12}	56.1×10^{-15}
$Z_{1/2}$	0.67	7.35×10^{12}	5.67×10^{-15}
$EH_{6/7}$	1.48	4.4×10^{11}	1.24×10^{-15}

- The usually observed trap centers Ti(c), $Z_{1/2}$, and $EH_{6/7}$ have been observed.
- The concentrations of the defects were found to be similar to that observed in our 20 µm thick 4H-SiC epilayers.

1. S. K. Chaudhuri, O. Karadavut, J. W. Kleppinger, and K. C. Mandal, *J. Appl. Phys.*, **130**, 074501, 2021.
2. J. W. Kleppinger, S. K. Chaudhuri, O. Karadavut, and K. C. Mandal, *Appl. Phys. Lett.*, **119**, 063502, 2021.

Defect Characterization (Ni/Ga_2O_3/4H-SiC MOS)

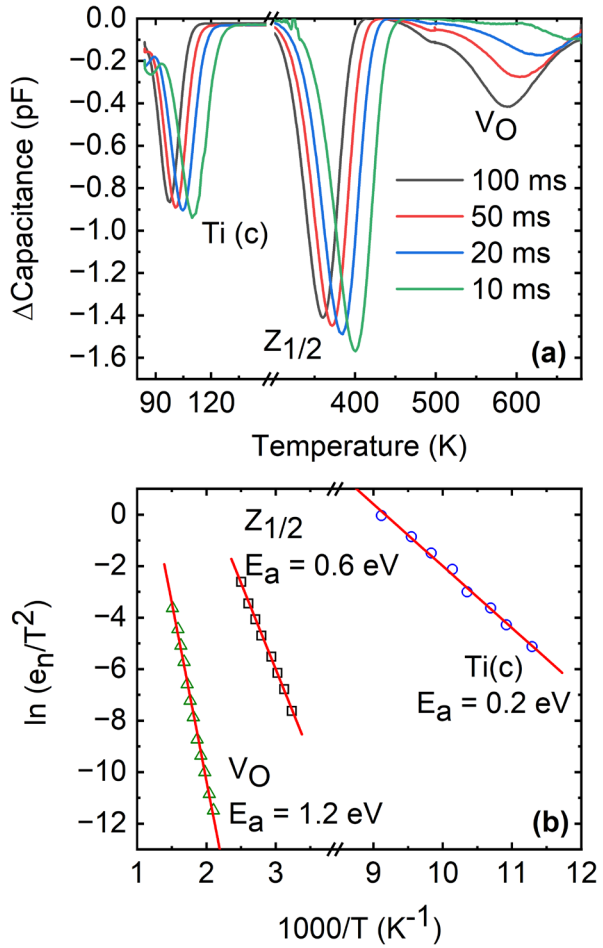

(a) DLTS spectra obtained for a 100 nm/20 μm thick Ni/β-Ga_2O_3/(n)4H-SiC SBD **(b)** The corresponding Arrhenius plots.

Trap Center	Activation Energy (eV)	Concentration (cm^{-3})	Capture cross-section (cm^2)
Ti (c)	0.20	5.22×10^{12}	4.89×10^{-13}
$Z_{1/2}$	0.60	8.89×10^{12}	2.14×10^{-16}
V_O	1.21	4.3×10^{12}	7.90×10^{-15}

- Three trap centers Ti(c) and $Z_{1/2}$ has been observed.
- $EH_{6/7}$ related to carbon vacancies are potential electron trap center were not observed.
- Instead, presence of V_O trap center in Ga_2O_3 has been observed.

Conclusions

- Wide bandgap radiation hard 4H-SiC detectors have been demonstrated as most suitable for harsh environment applications.
- 4H-SiC possesses material qualities that conventional semiconductors cannot provide, and 4H-SiC devices demonstrate performance at par with such detectors.
- No other wide bandgap semiconductor has the maturity level and manufacturing readiness level for harsh environment radiation detection.
- Apart from charged particle detection, 4H-SiC detectors, because of their wideband gap, have been demonstrated as excellent ultraviolet detectors.
- Modified MOS detector structure have been observed to enhance the device performance, especially for biasless operation and UV detection.
- Studies are underway to determine the UV responsivity using bias less 4H-SiC MOS detectors.

Acknowledgments

DOE Office of Nuclear Energy's Nuclear Energy University Programs (NEUP), Grant No. DE-NE0008662;

HSC Seed Grant, Prisma Health, Grant #10011863;

Transformative Research Seed Grant Initiative Award #80004827;

South Carolina NASA EPSCoR RGP, Grant # 10011935 ; and

NASA SCSG REAP program Grant #10013007.

THANK YOU

Correspondence:
Prof: Krishna C. Mandal: mandalk@cec.sc.edu